Accepted Manuscript

Title: Promotional Effect of Water in the Clean Continuous Production of Carvacrol from Carvone

Authors: Pedro Benavente, Fernando Cárdenas-Lizana, Mark A. Keane

Please cite this article as: Pedro Benavente, Fernando Cárdenas-Lizana, Mark A.Keane, Promotional Effect of Water in the Clean Continuous Production of Carvacrol from Carvone, Catalysis Today https://doi.org/10.1016/j.cattod.2017.09.059

This is a PDF file of an unedited manuscript that has been accepted for publication. As a service to our customers we are providing this early version of the manuscript. The manuscript will undergo copyediting, typesetting, and review of the resulting proof before it is published in its final form. Please note that during the production process errors may be discovered which could affect the content, and all legal disclaimers that apply to the journal pertain.

Promotional Effect of Water in the Clean Continuous Production of Carvacrol from Carvone
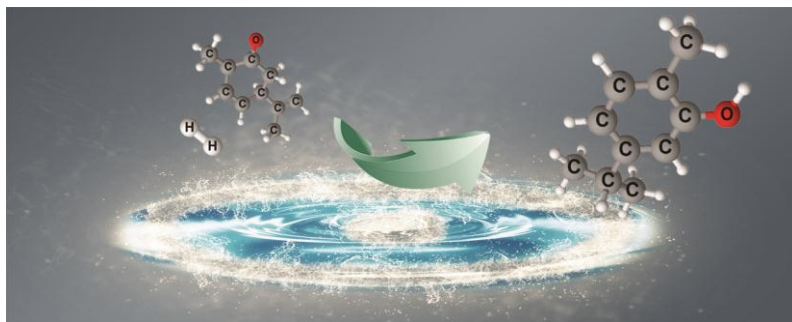
Pedro Benavente,

Fernando Cárdenas-Lizana* and Mark A. Keane

Chemical Engineering, School of Engineering and Physical Sciences,

Heriot-Watt University, Edinburgh EH14 4AS, Scotland

*corresponding author: tel.: +44(0)131 4514115,
e-mail: F.CárdenasLizana@hw.ac.uk

Graphical abstract

Highlights

- Ambient pressure continuous conversion of carvone to carvacrol over Pd/Al_2O_3.

- Hydrogenation to carvotanacetone/carvomenthone at H_2/carvone≥ 0.5.

- Exclusive isomerisation to carvacrol in H_2O.

- 100% yield of carvacrol in H_2 with H_2O as promoter.

Abstract

We have studied the effect of water on the selective conversion of biomass-derived carvone to carvacrol over Pd/Al_2O_3 (mean Pd size = 3 nm). Full selectivity to carvacrol was observed in H_2O (H_2O:Carvone = 1:12-6:1) without H_2 or at an inlet H_2:Carvone = 1:6. Carvacrol generation from carvone involves double bond migration with keto-enol tauromerisation. The formation of hydrogenation products (carvotanacetone and carvomenthone) was a feature of reaction at higher H_2 content. The incorporation of water (H_2O:Carvone $\leq$ 1:3) with hydrogen (H_2:Carvone = 1:6-2:1) increased carvacrol production rate to deliver 100% yield. A higher H_2O content lowered rate due to competition with carvone for surface active sites. Our results demonstrate the benefits of carvacrol production in continuous flow relative to conventional batch processes allowing full selective transformation under mild

reaction conditions.

1 Introduction

Biomass offers an alternative carbon source to supplant current dependence on crude oil and natural gas for the production of fine chemicals [1]. Biomass upgrading can enhance process sustainability but is still at an early stage of development [2]. The flavour and fragrance industry is based on terpenes [3], which are derived from the paper pulp and citric juice industries [4]. Natural terpenes contain -C=C- bonds and chemo-catalytic isomerisation can produce more valuable products [5]. Reviews by Swift in 2004 [3], Corma *et al.* in 2007 [5], Schwab and co-workers in 2013 [4] and Sanchez *et al.* in 2016 [6] covered terpene isomerisation by homogeneous catalysts in batch liquid systems where product selectivity was identified as the main challenge. Heterogeneous catalysis reduces separation costs and the volume of toxic waste [4] while operation in continuous flow offers clear benefits in terms of reduced downtime and higher throughput [7]. Carvacrol is a mono-terpenoid phenol used as a flavoring agent and intermediate for the production of drugs, fungicides and pesticides [6]. The main routes to carvacrol include (i) supercritical (300 bar) CO_2 extraction from oregano essential oils [8] and (ii) isopropylation of *o*-cresol with propylene over activated alumina at 50 bar and 633 K [9]. The requirements for high operating temperatures and pressures are major drawbacks. Carvacrol generation from carvone in hydrogen over supported metal catalysts is an alternative but studies to date are limited and inconclusive with work focused on batch systems in organic solvents (*e.g.* toluene, alcohols) [10-16].

Carvone transformation in hydrogen generates a range of products (**Figure 1**). The formation of unsaturated (carvotanacetone) and saturated (carvomenthone) ketones and alcohol (carvomenthol) occurs *via* path **(II)**; the endo-cyclic double bond and carbonyl functionalities are more resistant to attack [17,18]. We have reported the results of continuous catalytic carvone hydrogenation over bulk and (oxide and carbon) supported Pd catalysts where Pd/Al_2O_3 delivered the highest combined activity and carvacrol selectivity [19]. In that work, we established carvone → carvacrol transformation in hydrogen and a dependence of isomerisation (to carvacrol, path **(IA)** in **Figure 1**) *vs*. hydrogenation (path **(II)**) on H_2 content in the feed.

Water has been shown to impact on gas phase catalytic hydrogenation [20] and isomerisation mechanisms [21], which are critical steps in carvone transformation (**Figure 1**). A promoting effect of water has been reported in the hydrogenation (of *carbonyl* (acetone → isopropanol [22] and acetic acid → ethanol [20]) and *-C=C-* functionalities [23]) and isomerisation (oleic acid → isostearates [24,25]). We could not find any report that has examined the role of water in the catalytic transformation of a reactant containing both -C=C- and -C=O groups. Cao *et al.* [26] provided theoretical evidence that water can lower the energy barrier in the isomerisation of fulminic acid (HCNO) and isocyanic acid (HNCO). Water has, however, been found to have no effect or to inhibit hydrogenation (levulinic acid [27] and maleic anhydride [28]) and isomerisation (oleic acid [29]). In this study, we evaluate the effect of water in determining the selective continuous gas phase conversion of carvone to carvacrol over Pd/Al_2O_3.

2 Experimental

2.1 Catalyst Activation and Characterisation

A commercial (Sigma-Aldrich) 1.2% wt. Pd/Al_2O_3 was sieved to mean diameter = 75 μm and activated in 60 cm^3 min^{-1} H_2 at 10 K min^{-1} to 573 K. The sample was passivated in 1% v/v O_2/He at ambient temperature for *ex*-situ characterisation. Palladium content was measured by ICP-OES (Vista-Pro, Varian Inc.). Temperature programmed reduction (TPR, in 5% v/v H_2/N_2 at 10 K min^{-1} to 573 K), H_2 chemisorption (at 298 K) and total specific surface area (SSA, in 30% v/v N_2/He using the single point BET method) measurements were conducted on the commercial CHEM-BET 3000 (Quantachrome) unit as described elsewhere [30]; results were reproducible to ±7%. Bulk catalyst structure was determined by X-ray diffraction (XRD) analysis, using a Bruker/Siemens D500 incident X-ray diffractometer with Cu Kα radiation (0.02° $step^{-1}$ at 5 s $step^{-1}$ over the range 20° ≤ 2θ ≤ 90°). Palladium particle morphology was determined by scanning transmission electron microscopy (STEM, JEOL 2200FS field emission gun-equipped TEM), employing Gatan Digital Micrograph 1.82 for data acquisition/manipulation. Samples for analysis were crushed and deposited (dry) on a holey carbon/Cu grid (300 Mesh). Surface area-weighted mean Pd sizes (d) were measured from a count of 800 particles [30]. For comparison purposes, Pd size was also determined from H_2 chemisorption (at 298 K) [31] considering dissociative adsorption (Pd:H stoichiometry = 1:1) and assuming spherical morphology [32].

2.2 Catalytic Procedure

Carvone (98%), carvacrol (98%), dihydrocarvone (99%) and carveol (98%) were obtained from Sigma-Aldrich and used as supplied. Carvotanacetone, carvomenthone and carvomenthol were synthesised following published methods [33]. All gases (H_2, N_2, O_2 and He) were ultra-high purity (BOC, 99.9%). Reactions were conducted at atmospheric pressure and isothermal conditions (423 K) *in situ* after activation in a continuous flow fixed bed vertical tubular glass reactor (15 mm i.d.). A layer of borosilicate glass beads served as preheating zone where the organic reactant was vaporised and reached reaction temperature before contacting the catalyst. Temperature was continuously monitored by a thermocouple inserted in a thermowell within the catalyst bed. The organic reactant and H_2O were delivered *via* two glass/teflon air-tight syringes and teflon lines using two microprocessor controlled infusion pumps (Model 100 kd Scientific). A co-current flow of N_2, H_2 or H_2+N_2 with carvone (N_2:Carvone = 20:1 mol mol^{-1}, H_2:Carvone = 1:6 – 20:1 mol mol^{-1}) or H_2O+carvone (H_2O:Carvone = 1:12 – 6:1 mol mol^{-1}) was maintained at GHSV = 2 × 10^4 h^{-1}. Palladium (*n*) to reactant (*F*) molar ratio spanned the range 3 × 10^{-5} – 3 × 10^{-3} h. In blank tests, reactions in the absence of catalyst or over the Al_2O_3 support alone did not result in any measurable conversion. The reactor effluent was frozen in a liquid N_2 trap for analysis using a Perkin-Elmer Auto System XL gas chromatograph with split/splitless injector, FID and Stabilwax capillary column (RESTEK). Data acquisition/manipulation used the TotalChrom data system. Fractional carvone conversion (*X*) is given by:

7

$$X = \frac{[Carvone]_{in} - [Carvone]_{out}}{[Carvone]_{in}} \qquad (1)$$

with selectivity to carvacrol ($S_{Carvacrol}$):

$$S_{Carvacrol} (\%) = \frac{[Carvacrol]_{out}}{[Carvone]_{in} - [Carvone]_{out}} \times 100 \qquad (2)$$

Catalytic activity is also quantified in terms of carvacrol production rate (R, min^{-1}), extracted from time on-stream measurements [34]. Repeated reactions with different samples from the same batch of catalyst delivered raw data reproducibility and carbon mass balances within ±5%.

3 Results and discussion

3.1 Catalyst Characterization

The physico-chemical characteristics of the Pd/Al_2O_3 catalyst are given in **Table 1**. Temperature programmed reduction (TPR) generated the profile shown in **Figure 2(A)** with H_2 release (negative peak) at 375 K due to the decomposition of Pd hydride formed by room temperature H_2 absorption [35]. The XRD diffractogram of the activated catalyst (**Figure 2(B)**) shows two broad peaks at $2\theta = 45.8°$ and $66.8°$ characteristic of the main planes of cubic γ-Al_2O_3 (JCPDS-ICDD Card No. 10-0425). The total specific surface area (SSA = 145 m^2 g^{-1}) is consistent with γ-Al_2O_3 [36]. The absence of reflections due to Pd (main reflection at $2\theta = 40.1°$ for (111); JCPDS-ICDD Card No. 05-0681) suggests the presence of Pd nanoparticles (≤3 nm) below XRD detection limits [37]. A Pd particle size of 2.4 nm was obtained from H_2 chemisorption. The representative STEM image in **Figure 2(C)** further confirms the occurrence of Pd as nano-particles (≤6 nm, see **Figure 2(D)**) with a mean size of 3

8

nm.

3.2 Gas Phase Catalytic Conversion of Carvone

The formation of carvacrol can occur either *via* direct conversion of carvone (path **(IA)** in **Figure 1**) or through transformation of the carvotanacetone intermediate (path **(IB)**). There was no detectable carvone conversion for reaction in N_2 (without H_2 or H_2O), a result that deviates from the reported formation of several products (including carvacrol) over Pd/C in batch operation (for up to 12 h) at 506 K [38]. The shorter contact time (0.2 s) and lower reaction temperature (423 K) employed in this work did not result in carvone to carvacrol transformation in the absence of hydrogen or water in continuous gas phase operation.

At a low hydrogen content in the feed (H_2:Carvone = 1:6), we achieved full selectivity to carvacrol (**Figure 3(A)**) over Pd/Al$_2$O$_3$. This is an important result considering the reported low carvacrol selectivity ($\leq 38\%$) in batch systems over Pd catalysts [15,39]. To probe reaction pathway, carvone and carvotanacetone were used as reactants under the same reaction conditions. Negligible carvotanacetone conversion (<5%) for reaction over Pd/Al$_2$O$_3$ in H_2 suggests that carvacrol formation through path **(IB)** is not promoted. Carvacrol formation can proceed by carvone interaction with Pd sites *via* the exo -C=C- group [40] (**Figure 4(A)**). Dissociative adsorption of H_2 on Pd [41] generates reactive atomic hydrogen that attacks the exo-double bond. This results in the formation of an allyl intermediate that undergoes H elimination with bond migration and keto-enol tautomerisation to generate carvacrol [42,43]. At higher H_2:Carvone (= 1:2-20:1) the increase in surface hydrogen

9

from H_2 dissociation [44] favours H insertion [19] that directs the reaction along path (**II**) with the formation of carvontanacetone ($S_{Carvotanacetone} \leq 25\%$) and carvomenthone ($S_{Carvomenthone} \leq 10\%$).

Reaction in H_2O (without H_2) gave carvacrol as the only detected product. Strauss *et al.* [45,46] reported carvone isomerisation in water with no catalyst using a pressurised microwave batch reactor operated at 523 K. Water has been deemed essential for carvacrol isomerisation (at 373 K) with homogeneous Rh catalysts, where there was no conversion under anhydrous conditions; no explanation was provided to account for this [43]. We envision a reaction mechanism (**Figure 4(B)**) where water adsorbs associatively on Pd through the oxygen atom [22,47] and can coordinate with carvone, acting as both hydrogen donor and acceptor [21]. A surface water-carvone complex is formed with proton donation from O-H to the carbonyl-oxygen [48,49] and back donation from carvone to the water oxygen (Lewis base [21]). Enolisation of the carbonyl function favours aromatisation *via* migration of the isopropenyl double bond to generate carvacrol. A higher rate was evident for reaction in hydrogen (H_2:Carvone = 1:6) compared with water (in N_2, **Figure 3(B)**) where fractional carvone conversion was less than 0.15 and carvacrol production rate was insensitive to H_2O:Carvone molar ratio.

We considered the combined effect of H_2O and H_2 in terms of rate and carvacrol selectivity. Varying H_2O:Carvone (from pure carvone (0:1) to 1:3) under hydrogen lean conditions (H_2:Carvone = 1:6), reaction over Pd/Al_2O_3 was fully selective to carvacrol to give 100% yield (**Figure 3(A)**). The presence of H_2O served to

significantly raise carvacrol production rate (150 min^{-1} → 320 min^{-1}), which increased with increasing water content (**Figure 3(B)**). Ngo *et al.* [24] also reported water promotion in the isomerisation of oleic acid to isostearates over zeolites but they did not propose a possible cause. At H$_2$O:Carvone = 1:3, the rate was appreciably greater than that recorded for reaction in H$_2$ without H$_2$O (150 min^{-1}) or in H$_2$O without H$_2$ (35 min^{-1}). We propose that double bond migration following exo -C=C- bond hydrogen addition is facilitated by an increased reactivity of the ring due to water-assisted -C=O group enolisation with a resultant increase in carvacrol production rate. We examined the effect of water addition at higher H$_2$:Carvone (= 2:1) under conditions where hydrogenation is promoted ($S_{Cavotanacetone}$ = 14%). Incorporation of H$_2$O suppressed hydrogenation (path **(II)** in **Figure 1**) and shifted the reaction along path **(IA)** with exclusive isomerisation to carvacrol to reach 100% yield (**Figure 3(A)**). The coordination of water with carvone through the -C=O functionality favours ketone enolisation and inhibits carvotanacetone formation (path **(II)** (**Figure 1**)) directing the reaction to carvacrol *via* path **(IB)**, *i.e.* carvone isomerisation is promoted in water under conditions of excess hydrogen.

The rate of carvacrol production declined at a higher H$_2$O content (H$_2$O:Carvone > 1:3) regardless of H$_2$:Carvone (see **Figure 3(B)** for H$_2$:Carvone = 1:6), a result that suggests inhibited carvone uptake/activation due to competition for surface active sites. Chen *et al.* [22] demonstrated that increased surface coverage by water (≥5% coverage) lowers the heat of ketone adsorption, impeding activity. Our results demonstrate the advantages of switching from conventional batch systems to a

11

continuous catalytic process where: (i) the reaction can be operated under mild reaction conditions (423 K and atmospheric pressure); (ii) 100% yield of carvacrol is achieved in a hydrogen lean feed with water as promoter; (iii) sole formation of cavacrol reduces production costs associated with downstream separation of undesired by-products.

4 Conclusions

We have evaluated the promotional effect of H_2O in the continuous gas phase conversion of carvone to carvacrol over Pd/Al_2O_3 (mean Pd size = 3 nm from STEM). Exclusive carvacrol formation was observed in H_2O and an inlet H_2:Carvone = 1:6. At higher H_2 content (H_2:Carvone = 1:2-20:1), hydrogenation to carvotanacetone and carvomenthone was promoted. Where H_2O:Carvone ≤ 1:3 (at H_2:Carvone = 1:6-2:1), carvacrol production rate was greater than conversion in hydrogen alone to give 100% carvacrol yield. This is linked to the effect of water on keto-enol tauromerisation that favours double bond migration. Higher H_2O content (H_2O:Carvone > 1:3) lowered activity due to competition for surface sites with carvone. The results of this work establish viable use of water to promote continuous isomerisation and enable full transformation of carvone to carvacrol.

Acknowledgements

References

[1]   Y. Jiang, X. Wang, Q. Cao, L. Dong, J. Guan, X. Mu, in: M. Xian (Ed.),

Sustainable Production of Bulk Chemicals, Springer Netherlands, Dordrecht, 2016, pp. 19-49.

[2] Z. Ma, L. Wei, W. Zhou, L. Jia, B. Hou, D. Li, Y. Zhao, RSC Adv. 5 (2015) 88287-88297.

[3] K. A. D. Swift, Top. Catal. 27 (2004) 143-155.

[4] W. Schwab, C. Fuchs, F.-C. Huang, Eur. J. Lipid Sci. Technol. 115 (2013) 3-8.

[5] A. Corma, S. Iborra, A. Velty, Chem. Rev. 107 (2007) 2411-2502.

[6] L. M. Sanchez, H. J. Thomas, M. J. Climent, G. P. Romanelli, S. Iborra, Catal. Rev. 58 (2016) 497-586.

[7] I. M. Mándity, S. B. Ötvös, F. Fülöp, ChemistryOpen 4 (2015) 212-223.

[8] A. Ocaña-Fuentes, E. Arranz-Gutiérrez, F. J. Señorans, G. Reglero, Food Chem. Toxicol. 48 (2010) 1568-1575.

[9] G. D. Yadav, S. B. Kamble, J. Chem. Technol. Biotechnol. 84 (2009) 1499-1508.

[10] I. M. J. Vilella, S. R. de Miguel, O. A. Scelza, J. Mol. Catal. A: Chem. 284 (2008) 161-171.

[11] C. I. Melo, R. Bogel-Łukasik, E. Bogel-Łukasik, J. Supercrit. Fluid. 61 (2012) 191-198.

[12] S. R. de Miguel, M. C. Román-Martínez, D. Cazorla-Amorós, E. L. Jablonski, O. A. Scelza, Catal. Today 66 (2001) 289-295.

[13] G. C. Torres, S. D. Ledesma, E. L. Jablonski, S. R. de Miguel, O. A. Scelza, Catal. Today 48 (1999) 65-72.

[14] S. R. de Miguel, M. C. Román-Martínez, E. L. Jablonski, J. L. G. Fierro, D. Cazorla-Amorós, O. A. Scelza, J. Catal. 184 (1999) 514-525.

[15] E. I. Klabunovskii, L. F. Godunova, L. K. Maslova, B. Acad. Sci. USSR Chem. Sci. 21 (1972) 1020-1024.

[16] C. I. Melo, Alternative Solvents in Carvone Hydrogenation, Chemical Engineering, Universidade Nova de Lisboa, Lisbon (2011) pp. 53.

[17] R. A. Kjonaas, S. P. Mattingly, J. Chem. Educ. 82 (2005) 1813-1814.

[18] P. Barbaro, F. Liguori, Heterogenized Homogeneous Catalysts for Fine

Chemicals Production: Materials and Processes, Springer, Dordrecht, 2010.

[19] P. Benavente, F. Cárdenas-Lizana, M. A. Keane, Catal. Commun. 96 (2017) 37-40.

[20] H. Olcay, Y. Xu, G. W. Huber, Green Chem. 16 (2014) 911-924.

[21] E. Bosch, J. M. Lluch, J. Bertran, Can. J. Chem. 68 (1990) 666-673.

[22] H. Chen, J. Zhao, S. Li, J. Xu, J. Shen, Chin. J. Catal. 36 (2015) 380-388.

[23] L. Nikoshvili, E. Shimanskaya, A. Bykov, I. Yuranov, L. Kiwi-Minsker, E. Sulman, Catal. Today 241, Part B (2015) 179-188.

[24] H. L. Ngo, A. Nuñez, W. Lin, T. A. Foglia, Eur. J. Lipid Sci. Technol. 109 (2007) 214-224.

[25] T. Tomifuji, H. Abe, Y. Matsumura, Y. Sakuma, Process for the Preparation of Branched Chain Fatty Acids and Alkyl Esters Thereof, US5677473 A, 1997.

[26] J. Cao, Z. X. Wang, L. J. Gao, F. Fu, J. Mol. Model. 21 (2015) 66/01-66/08.

[27] W. Bonrath, A. M. C. F. Castelijns, J. G. de Vries, R. P. M. Guit, J. Schütz, N. Sereinig, H. W. L. M. Vaessen, Catal. Lett. 146 (2016) 28-34.

[28] Y. Yu, W. Zhan, Y. Guo, G. Lu, S. Adjimi, Y. Guo, J. Mol. Catal. A: Chem. 395 (2014) 392-397.

[29] L. Ha, J. Mao, J. Zhou, Z. C. Zhang, S. Zhang, Appl. Catal. A: Gen. 356 (2009) 52-56.

[30] M. Li, X. Wang, Y. Hao, F. Cárdenas-Lizana, M. A. Keane, Catal. Today 279 (2017) 19-28.

[31] F. Cárdenas-Lizana, D. Lamey, S. Gómez-Quero, N. Perret, L. Kiwi-Minsker, M. A. Keane, Catal. Today 173 (2011) 53-61.

[32] F. Cárdenas-Lizana, Y. Hao, M. Crespo-Quesada, I. Yuranov, X. Wang, M. A. Keane, L. Kiwi-Minsker, ACS Catal. 3 (2013) 1386-1396.

[33] C. Petrier, J.-L. Luche, Tetrahedron Lett. 28 (1987) 2351-2352.

[34] M. Li, Y. Hao, F. Cárdenas-Lizana, H. H. P. Yiu, M. A. Keane, Top. Catal. 58 (2015) 149-158.

[35] L. L. Jewell, B. H. Davis, Appl. Catal. A: Gen. 310 (2006) 1-15.

[36] I. Chorkendorff, J. W. Niemantsverdriet, Concepts of Modern Catalysis and

Kinetics, Wiley-VCH, Weinheim, 2003.

[37]   J. Liu, Microsc. Microanal. 10 (2004) 55-76.

[38]   E. C. Horning, J. Org. Chem. 10 (1945) 263-266.

[39]   C. I. Melo, R. Bogel-Łukasik, M. G. da Silva, E. Bogel-Łukasik, Green Chem. 13 (2011) 2825-2830.

[40]   A. M. Doyle, S. K. Shaikhutdinov, H. J. Freund, J. Catal. 223 (2004) 444-453.

[41]   G. Prelazzi, M. Cerboni, G. Leofanti, J. Catal. 181 (1999) 73-79.

[42]   W. Ludwig, A. Savara, S. Schauermann, Dalton Trans. 39 (2010) 8484-8491.

[43]   H. M. Colquhoun, J. Holton, D. J. Thompson, M. V. Twigg, New Pathways for Organic Synthesis: Practical Applications of Transition Metals, Springer US, New York, 2012.

[44]   S. J. Blanksby, G. B. Ellison, Acc. Chem. Res. 36 (2003) 255-263.

[45]   J. An, L. Bagnell, T. Cablewski, C. R. Strauss, R. W. Trainor, J. Org. Chem. 62 (1997) 2505-2511.

[46]   X.-J. Bi, L. T. Higham, J. L. Scott, C. R. Strauss, Aust. J. Chem. 59 (2006) 883-886.

[47]   J. M. Heras, G. Estiú, L. Viscido, Appl. Surf. Sci. 108 (1997) 455-464.

[48]   H. Wan, A. Vitter, R. V. Chaudhari, B. Subramaniam, J. Catal. 309 (2014) 174-184.

[49]   B. Ren, M. Zhao, L. Dong, G. Li, Catal. Commun. 50 (2014) 92-96.

Figures

Figure 1: Reaction pathways in the conversion of carvone to (target) carvacrol (**path I**, solid arrows), carvomenthol (**path II**, open arrows), dihydrocarvone (**path III**, dashed arrow) and carveol (**path IV**, dotted arrow).

Figure 2: (A) TPR profile, **(B)** XRD diffractogram with main planes for γ-Al_2O_3 from JCPDS-ICDD reference (Card No. 10-0425) and **(C)** representative STEM image with **(D)** Pd particle size distribution for Pd/Al_2O_3.

Figure 3: (A) Carvacrol selectivity ($S_{Carvacrol}$, %) as a function of fractional conversion (X) of carvone and **(B)** variation in carvacrol production rate (R, min^{-1}) with inlet H_2O:Carvone molar ratio for reactions in H_2 (H_2:Carvone = 1:6 (□) and = 1:2-20:1 (△)) and H_2O (H_2O:Carvone = 1:12-1:6 in N_2 (✚) and in H_2 (H_2:Carvone = 1:6, ⊞ and = 2:1, ⊕)). *Note*: Arrows in **(A)** illustrate $S_{Carvacrol}$ *vs. X* dependence for reactions with increased H_2 in the feed (dotted line) and the effect of adding water for reactions in N_2 (solid line) at H_2:Carvone = 1:6 (dashed line) and 2:1 (dashed-dotted line). *Reaction conditions*: $T = 423$ K, $n/F = 3 \times 10^{-5}$ $- 3 \times 10^{-3}$ h, GHSV = 2×10^4 h^{-1}.

Figure 4: Proposed carvone adsorption/activation and reaction with **(A)** H_2 and **(B)** H_2O.

Figure 1
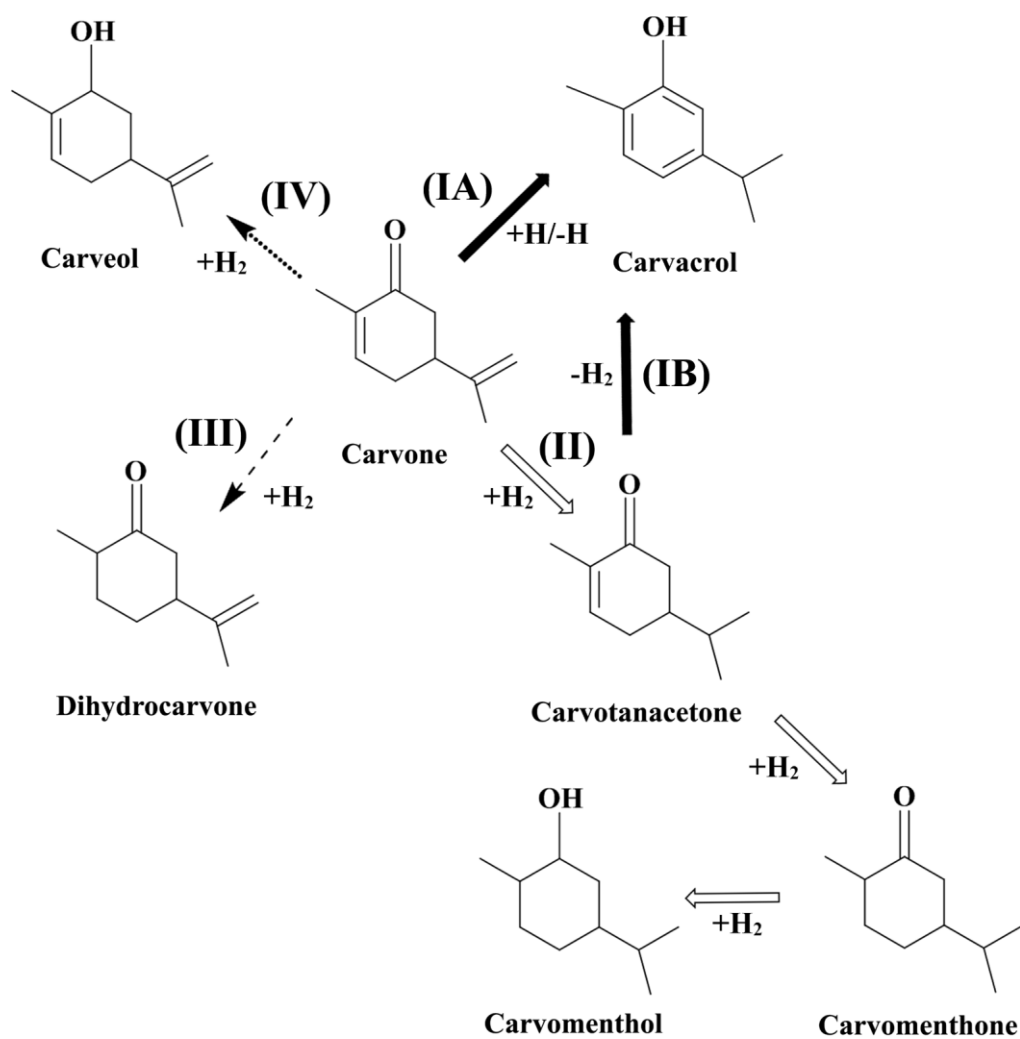
Figure 2
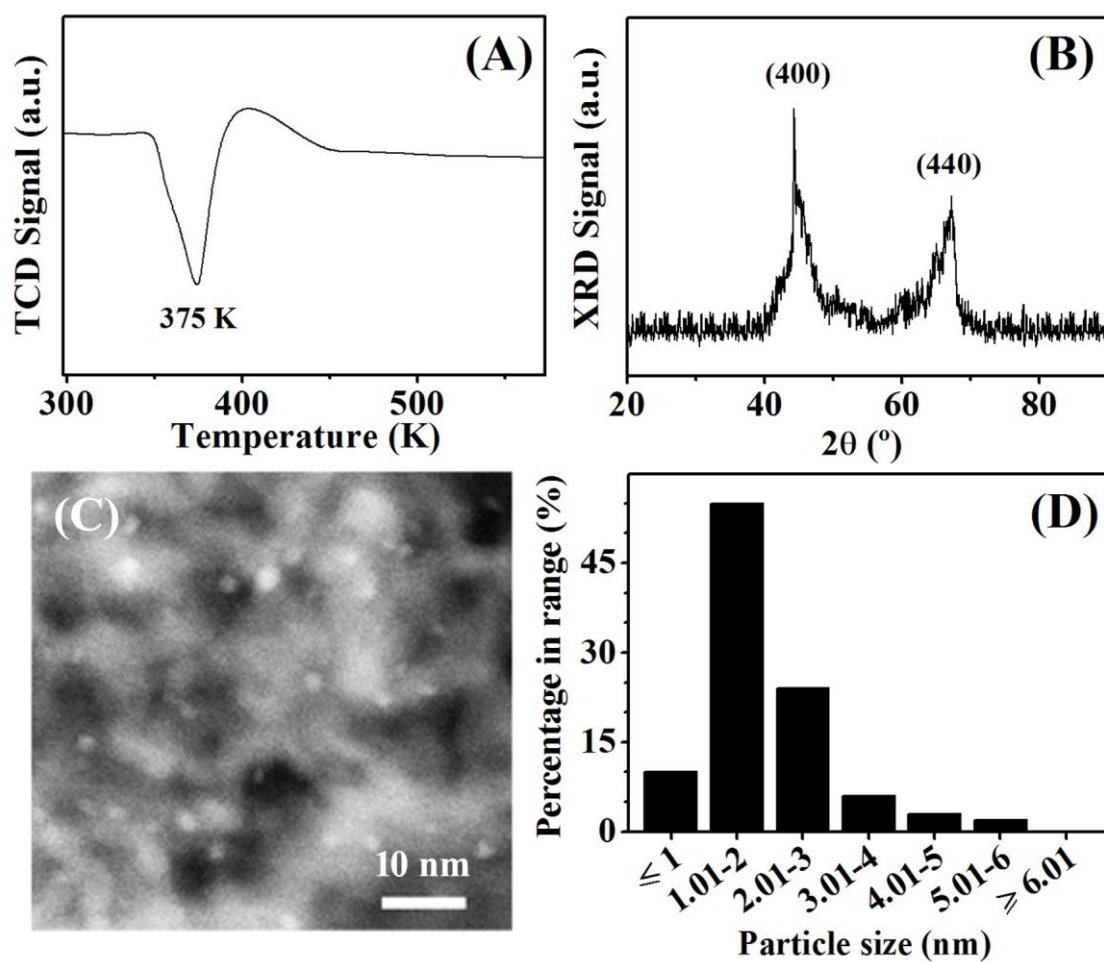
Figure 3
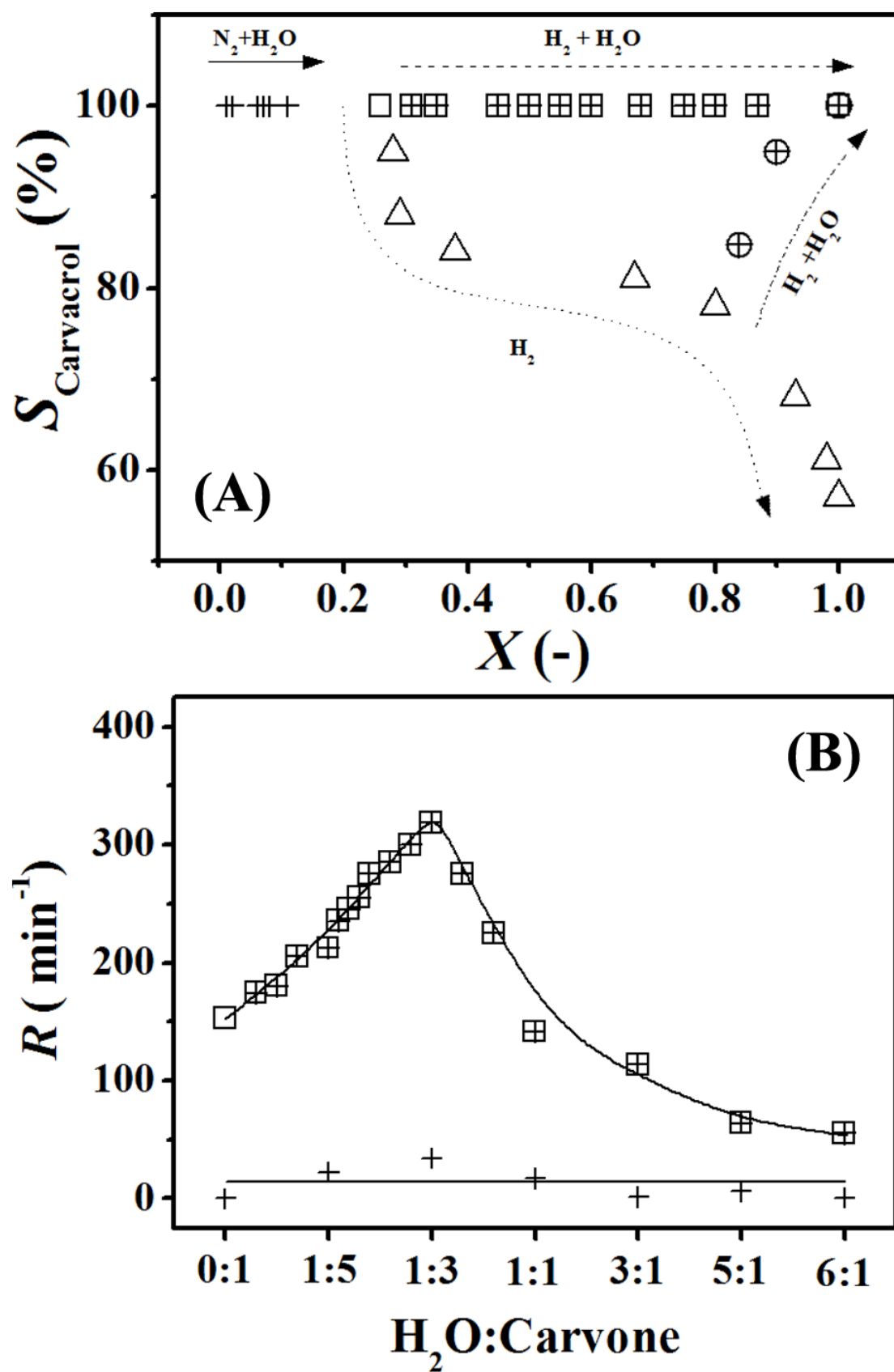
Figure 4
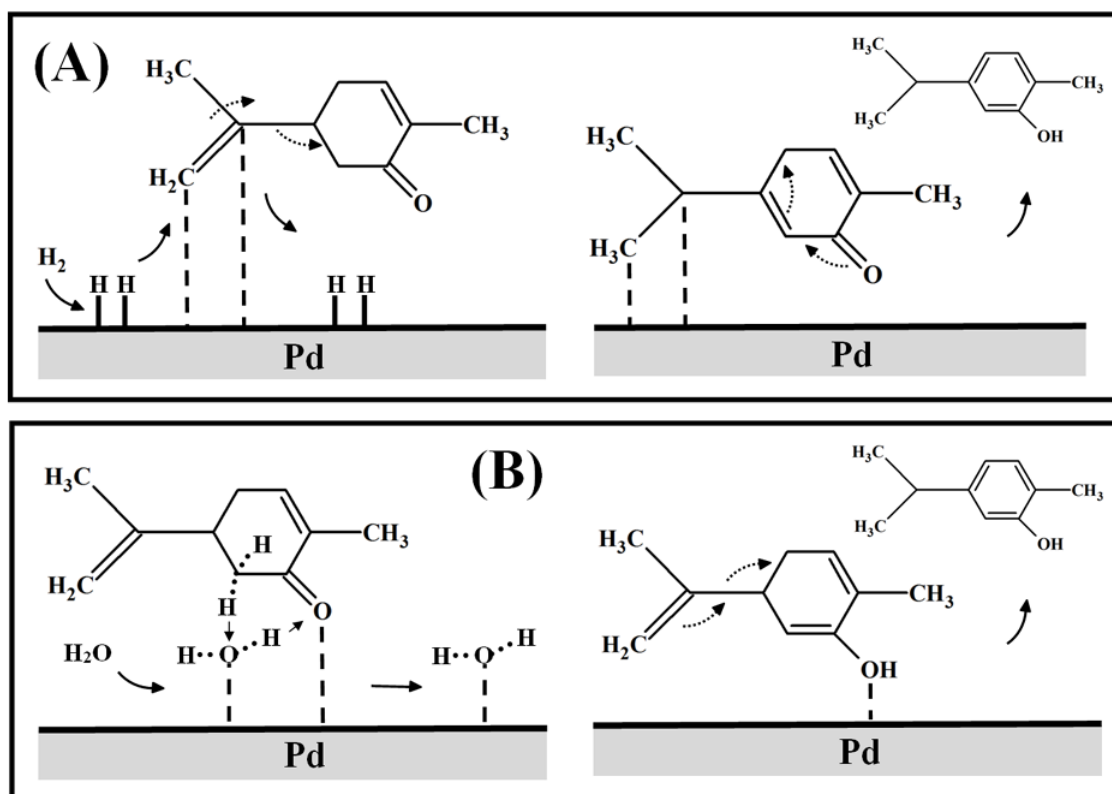
Table 1: Physico-chemical characteristics of the Pd/Al_2O_3 catalyst.

Pd loading (% wt.)	1.2
SSA ($m^2\ g^{-1}$)	145
TPR T_{max} (K)	375
Pd mean size (nm)	2.4^a / 3.0^b

[a]from H_2 chemisorption at 298 K.

[b]from STEM analysis (d).